Published online 19 September 2016 *Nucleic Acids Research, 2017, Vol. 45, No. 3* ***1479–1487***
doi: 10.1093/nar/gkw830

The loss of a hydrogen bond: Thermodynamic contributions of a non-standard nucleotide

Elizabeth A. Jolley and Brent M. Znosko*

Department of Chemistry, Saint Louis University, St Louis, MO 63103, USA

Received April 08, 2016; Revised September 07, 2016; Accepted September 08, 2016

ABSTRACT

Non-standard nucleotides are ubiquitous in RNA. Thermodynamic studies with RNA duplexes containing non-standard nucleotides, whether incorporated naturally or chemically, can provide insight into the stability of Watson–Crick pairs and the role of specific functional groups in stabilizing a Watson–Crick pair. For example, an A-U, inosine•U and pseudouridine•A pair each form two hydrogen bonds. However, an RNA duplex containing a central I•U pair or central Ψ•A pair is 2.4 kcal/mol less stable or 1.7 kcal/mol more stable, respectively, than the corresponding duplex containing an A-U pair. In the non-standard nucleotide purine, hydrogen replaces the exocyclic amino group of A. This replacement results in a P•U pair containing only one hydrogen bond. Optical melting studies were performed with RNA duplexes containing P•U pairs adjacent to different nearest neighbors. The resulting thermodynamic parameters were compared to RNA duplexes containing A-U pairs in order to determine the contribution of the hydrogen bond involving the exocyclic amino group. Results indicate a loss of 1.78 kcal/mol, on average, when an internal P•U replaces A-U in an RNA duplex. This value is compared to the thermodynamics of a hydrogen bond determined by similar methods. Nearest neighbor parameters were derived for use in free energy and secondary structure prediction software.

INTRODUCTION

RNA is an important biomolecule adopting a broad range of structures, which in turn provides a broad array of functionality. Whether found as mRNA, tRNA, or rRNA, the folding and structure of RNA play a crucial role in its observed biological function. The function of RNA is linked to its tertiary structure that extends from its secondary structure. Knowing or being able to predict the secondary and tertiary structure of RNA may therefore provide insight into the function or role of a specific RNA molecule. Prediction of tertiary structure from secondary structure can be a useful tool as the number of solved RNA structures climbs slowly, while the need for structure information grows quickly. In order to aid in the prediction of tertiary structure, there is a need to more fully understand secondary structure motifs, as well as non-canonical or non-Watson–Crick pairs.

Non-standard nucleotides occur naturally throughout RNA, but they can also be inserted purposefully into RNAs of interest. The use of non-standard nucleotides and their effect on duplex stability has been studied to help further understand the secondary structure of RNA (1–13). The approach of using non-standard nucleotides that have altered bases can also highlight the role of certain functional groups. Grohman *et al*. (6) explored the mechanism of folding directed by an RNA chaperone. The study made use of the non-standard nucleotide inosine in place of the native guanosine, and thus the loss of the exocyclic amino group, to help explain the mechanism of the folding process.

Purine (P), also known as nebularine, is a purine ring possessing no additional functional groups (Figure 1). Due to its structural similarity to (A), P has been used to probe structures to highlight the effects of base modifications on function. For example, P has been used to investigate the activity of adenosine deaminase enzymes (14,15). A-U pairs in RNA duplexes were replaced with P•U pairs, and the effect on enzyme activity was determined (14–18). In these studies, both with P and its analogues, the loss of the functional group inhibited the function of enzymes that recognize A (14–18). This inhibitory effect could be the result of the enzyme requiring the exocyclic amino group for function or could be the result of decreased stability in the target RNAs due to the A to P replacement.

Similarly, P has also been used to investigate hammerhead ribozyme cleavage (19–21) by replacement of A with P. The goal of replacement is to correlate a single functional group with a catalytic event (22). Commonly, the modified nucleotides selected to measure the cleavage rate have multiple functional group changes or deletions (22). P was chosen as a good candidate for replacement of A, since the only

*To whom correspondence should be addressed. Tel: +1 314 977 8567; Fax: +1 314 977 2521; Email: znoskob@slu.edu
Present address: Brent M. Znosko, Department of Chemistry, Saint Louis University, St Louis, MO 63103, USA.

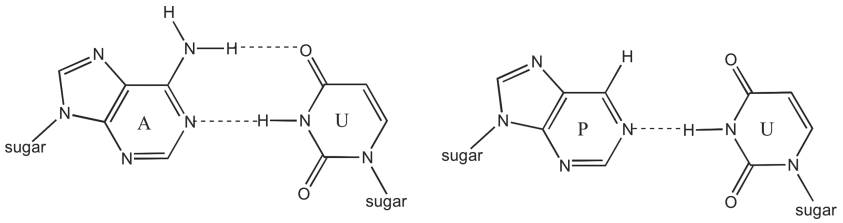

Figure 1. Structure of an A-U pair (left) and P•U pair (right).

structural difference between P and A is the exocyclic amino group of A, which only slightly changes the distribution of partial charges (7). The loss of the amino group at specific positions within the structure of the hammerhead ribozyme revealed a decrease in the cleavage reaction of the ribozyme (19–21). It is noted that the replacement took place at non-base pairing positions in the ribozyme. One study reported that the base stacking of the adjacent nucleotides with P was expected to be unaffected, although this was never tested or confirmed (19).

Blount *et al*. (22) acknowledged that a nucleotide modification may have consequences beyond hydrogen bonding ability and could alter properties such as stacking affinity and pKa. This has been confirmed in a study by Znosko *et al*. (7) where the contribution of the A amino group was explored in tandem A•A pairs. In the study, P replaced A at either one or both positions in the tandem pair. The pKa values for A and P were indeed different and were reported as 3.5 and 2.1, respectively. Although the study resulted in hydrogen bonds that were longer in 5′-PA-3′/3′-AP-5′, the study also reported that the duplex containing 5′-PA-3′/3′-AP-5′ was 1.3 kcal/mol more stable than the duplex containing 5′-AA-3′/3′-AA-5′. This thermodynamic difference can be explained by differences in the conformations adopted by these two motifs and differences in stacking interactions. The favorable stacking interaction in the duplex containing 5′-PA-3′/3′-AP-5′ may be strong enough to compensate for the longer hydrogen bonding. Performing a systematic thermodynamic investigation would aid in understanding the effect of P incorporation on duplex stability, specifically for P•U pairs.

Although not systematic, one previous study did look at the thermodynamic stability of RNA duplexes that incorporated non-standard nucleotides (23). Modified nucleotides, which included P, were introduced in place of various nucleotides for improved potency of siRNA (23). Addepalli *et al*. (23) set out to explore the effect of thermally destabilized RNA strands in order to find duplexes that dissociate prior to cleavage (23). Although this study did thermodynamically investigate the incorporation of P into RNA duplexes, it only investigated four duplexes (23). These data were not included in the analysis done here as each of the oligoribonucleotides had additional deoxynucleotides at the 3′ terminus.

In order to further the understanding of secondary structures of RNAs containing non-standard nucleotides, the thermodynamic contribution of P in RNA duplexes was systematically investigated. The results of this study highlight the effect P has on the stability of RNA duplexes, and in turn highlight the importance of the exocyclic amino group of A to duplex stability. The value of a hydrogen bond in the context of the duplexes studied here is compared to values derived from similar methods. Through this process, nearest neighbor parameters that can be implemented in secondary structure prediction software were also derived.

MATERIALS AND METHODS

Sequence design, synthesis, and purification

Duplexes were designed to give all combinations of nearest neighbors containing a P•U pair. These combinations were inserted into G-C rich stems to prevent fraying, resulting in duplexes that are 7 base pairs in length for the 16 duplexes containing P•U internal pairs and 6 base pairs in length for the 8 duplexes containing P•U terminal pairs. The sequences were entered into the structure prediction software *RNAstructure* (24) to check for possible competing structures. As *RNAstructure* (24) does not recognize P, A was used in its place for each of the sequences. Oligoribonucleotides containing P were synthesized and deprotected by the Keck lab at Yale University (New Haven, CT, USA), while complementary strands were obtained from Integrated DNA Technologies, Inc. Purification of the oligoribonucleotides followed standard TLC and column chromatography procedures (1,2).

Concentration calculations and duplex formation

Following a previously described method (1,2), RNA single strand concentrations were determined using Beer's law. Extinction coefficients for single strands were calculated using *RNACalc* (25), substituting the extinction coefficient of A for P. This replacement is justified as in some cases, the practice of replacing the extinction coefficient of a non-standard nucleotide with the extinction coefficient of the corresponding canonical nucleotide is common (1,2,23), yet in other cases, an average of the extinction coefficient of each standard nucleotide is used in place of the nonstandard nucleotide (23). Chen *et al*. (26) performed UV melting experiments with a duplex containing a P in place of an A. Here, the extinction coefficient of A was used for the extinction coefficient of P with the explanation that although there are differences in extinction coefficients due to functional group changes or deletions, the individual nucleotides only slightly contribute to the overall oligomer extinction coefficient and so the effect on thermodynamic measurements are minimal (26). Absorbance readings for the single strands and duplexes were taken at a temperature above 80°C to minimize unwanted folding of the RNA. Duplexes were formed

in a 1:1 molar ratio of single strands. Sample volumes, designed to give absorbance values between 0.2 and 2, were dried down and reconstituted in 100 μl of melt buffer (1 M sodium chloride, 20 mM sodium cacodylate, and 0.5 mM disodium EDTA at pH 7.0).

Optical melting

Optical melting experiments followed a scheme consisting of nine melts resulting from three concentrations subjected to a series of dilutions. This melt scheme gives a concentration range of at least 50-fold. The experiments were performed on a Beckman–Coulter DU800 spectrophotometer at 280 nm with a Beckman–Coulter high performance temperature controller using a heat rate of 1°C/min from 10–90°C.

Determination of thermodynamic parameters from optical melting

The optical melt curves were analyzed in *Meltwin* (25), which fits the melt curves to a two-state model, assuming linear sloping baselines and temperature independent values for enthalpy and entropy (25,27). *Meltwin* (25) requires the sequence in order to calculate thermodynamic parameters. The sequences were entered into *Meltwin* (25) with all P's being replaced with A's, therefore using the A extinction coefficient for P (see explanation above). T_M values were calculated at various concentrations to determine thermodynamic parameters, according to a previously described method by Borer *et al*. (28). Values from the melt curve fits were in good agreement with the van't Hoff plots (T_M versus log C_T), and so only values from the van't Hoff plots were used for further analysis.

Determination of P•U pair contribution to duplex thermodynamics

The nearest neighbor model was used to isolate the thermodynamic contribution of P•U pairs from the total RNA duplex contribution. Each duplex's thermodynamic contribution can be written as a sum of the nearest neighbor interactions. For example,

$$\Delta G^\circ_{37}\begin{pmatrix} GCAPAGC \\ CGUUUCG \end{pmatrix} = \Delta G^\circ_{37,i} + \Delta G^\circ_{37}\begin{pmatrix} GC \\ CG \end{pmatrix} + \Delta G^\circ_{37}\begin{pmatrix} CA \\ GU \end{pmatrix} + \Delta G^\circ_{37}\begin{pmatrix} AP \\ UU \end{pmatrix} + \Delta G^\circ_{37}\begin{pmatrix} PA \\ UU \end{pmatrix} + \Delta G^\circ_{37}\begin{pmatrix} AG \\ UC \end{pmatrix} + \Delta G^\circ_{37}\begin{pmatrix} GC \\ CG \end{pmatrix} \quad (1)$$

$\Delta G^\circ_{37}\left(\begin{smallmatrix} GCAPAGC \\ CGUUUCG \end{smallmatrix}\right)$ is the Gibbs free energy change for the duplex determined from optical melting, $\Delta G^\circ_{37,\,i}$ is the free energy change for duplex initiation determined to be 4.09 kcal/mol (29) and all other terms are the incremental nearest neighbor interactions. The sum of the P•U nearest neighbor interactions was determined by subtracting the canonical incremental interactions from the experimental duplex free energy (29). For example,

$$\Delta G^\circ_{37}\begin{pmatrix} AP \\ UU \end{pmatrix} + \Delta G^\circ_{37}\begin{pmatrix} PA \\ UU \end{pmatrix} = \Delta G^\circ_{37}\begin{pmatrix} GCAPAGC \\ CGUUUCG \end{pmatrix} - \Delta G^\circ_{37,\,i} - \Delta G^\circ_{37}\begin{pmatrix} GC \\ CG \end{pmatrix} - \Delta G^\circ_{37}\begin{pmatrix} CA \\ GU \end{pmatrix} - \Delta G^\circ_{37}\begin{pmatrix} AG \\ UC \end{pmatrix} - \Delta G^\circ_{37}\begin{pmatrix} GC \\ CG \end{pmatrix} \quad (2)$$

Similar calculations were performed for terminal P•U pairs, yielding one P•U nearest neighbor parameter instead of the summation of two. This same analysis was performed to derive ΔH° and ΔS° contributions from the P•U nearest neighbors.

Linear regression and determination of linearly independent P•U nearest neighbor values

The eight possible internal P•U nearest neighbor combinations plus a terminal combination were used as variables for linear regression using the LINEST function in *Microsoft Excel*, with the P•U contributions to ΔG°_{37} derived from Equation (2) used as constants. The LINEST function simultaneously solved for each variable and resulted in linearly independent nearest neighbor parameters. This same analysis was performed to derive P•U nearest neighbor values for ΔH° and ΔS°.

RESULTS

Thermodynamic parameters of duplexes containing P•U pairs

Table 1 lists the thermodynamic parameters of duplex formation derived from both van't Hoff plots (T_M^{-1} versus log (C_T/4)) and fitting the optical melting curves to a two-state model. Two duplexes, $\left(\begin{smallmatrix} PCGCGC \\ UGCGCG \end{smallmatrix}\right)$ and $\left(\begin{smallmatrix} PUGCGC \\ UACGCG \end{smallmatrix}\right)$, did not show single, sharp transitions during melting and were not included in any analysis including trends, averages or linear regression. The remaining duplexes did show single, sharp transitions and the enthalpy values derived from the average of curve fitting and the van't Hoff plots agree within 15% of each other, suggesting that a two-state transition occurred during duplex melting (30). A representative melt curve and van't Hoff plot can be found in Supplementary Data Figures S1 and S2.

Free energy comparison between duplexes containing P•U and A-U pairs

Table 2 lists the ΔG°_{37} measured from optical melting experiments of duplexes containing a P•U pair compared to the ΔG°_{37} from nearest neighbor calculations of the same duplex with an A-U pair replacing the P•U pair. Duplexes containing an internal P•U pair were, on average, 1.78 kcal/mol less stable than the corresponding duplex with an internal A-U pair, while duplexes containing a terminal P•U pair were 1.42 kcal/mol less stable, on average, than the corresponding duplex with a terminal A-U pair. Similar calculations and comparisons were done for enthalpy and entropy values, and these can be found in Supplementary Data Tables S1 and S2.

Table 1. Thermodynamic parameters of duplex formation

	T_M^{-1} versus log (C_T/4) plots				Average of curve fits				Predicted using new P·U NN parameters[d]			
oligomers[a]	ΔH° (kcal/mol)	ΔS° (eu)	ΔG°_{37} (kcal/mol)	T_M[b] (°C)	ΔH° (kcal/mol)	ΔS° (eu)	ΔG°_{37} (kcal/mol)	T_M[b] (°C)	ΔH° (kcal/mol)	ΔS° (eu)	ΔG°_{37} (kcal/mol)	T_M[b] (°C)
Internal												
GCAPAGC CGUUUCG	−75.1 ± 3.9	−219.9 ± 12.8	−6.95 ± 0.05	38.7	−72.6 ± 10.6	−211.5 ± 34.0	−7.03 ± 0.03	39.1	−71.5	−207.2	−7.19	40.0
GCAPCGC CGUUGCG	−76.8 ± 3.3	−219.2 ± 10.6	−8.84 ± 0.08	46.6	−71.6 ± 8.7	−202.7 ± 27.5	−8.75 ± 0.29	46.9	−76.9	−219.7	−8.77	46.4
GCAPGGC CGUUCCG	−74.0 ± 4.2	−207.8 ± 13.1	−9.55 ± 0.16	50.2	−73.4 ± 7.7	−205.9 ± 24.2	−9.58 ± 0.21	50.4	−78.5	−222.2	−9.57	49.5
GCAPUGC CGUUACG	−76.9 ± 5.8	−225.6 ± 18.6	−6.99 ± 0.10	38.9	−70.1 ± 16.7	−203.2 ± 53.5	−7.07 ± 0.21	39.4	−72.9	−213.1	−6.86	38.4
GCCPAGC CGGUUCG	−71.1 ± 2.1	−199.7 ± 6.5	−9.17 ± 0.06	49.0	−69.0 ± 4.5	−193.0 ± 14.4	−9.15 ± 0.09	49.2	−72.8	−203.9	−9.53	50.6
GCCPCGC CGGUGCG	−76.5 ± 1.9	−211.5 ± 5.9	−10.94 ± 0.10	55.9	−77.6 ± 2.1	−214.6 ± 6.5	−11.00 ± 0.10	56.0	−78.3	−216.4	−11.11	56.5
GCCPGGC CGGUCCG	−80.4 ± 2.4	−220.3 ± 7.2	−12.10 ± 0.15	60.1	−81.5 ± 1.4	−223.5 ± 4.2	−12.16 ± 0.07	60.0	−79.8	−218.9	−11.91	59.5
GCCPUGC CGGUACG	−79.0 ± 6.3	−225.0 ± 19.8	−9.21 ± 0.24	47.9	−75.6 ± 11.2	−214.1 ± 35.4	−9.17 ± 0.34	48.2	−74.3	−209.8	−9.20	48.6
GCGPAGC CGCUUCG	−71.1 ± 4.1	−200.4 ± 12.7	−8.99 ± 0.14	48.1	−74.4 ± 4.6	−210.6 ± 14.5	−9.11 ± 0.13	48.1	−71.9	−202.8	−8.97	47.9
GCGPCGC CGCUGCG	−76.0 ± 9.1	−210.5 ± 27.8	−10.69 ± 0.52	54.9	−75.6 ± 4.1	−209.4 ± 12.6	−10.69 ± 0.28	55.0	−77.3	−215.3	−10.55	54.0
GCGPGGC CGCUCCG	−79.7 ± 4.3	−218.7 ± 13.1	−11.89 ± 0.28	59.3	−79.7 ± 9.8	−219.0 ± 29.4	−11.83 ± 0.67	59.1	−78.9	−217.8	−11.35	57.1
GCGPUGC CGCUACG	−79.2 ± 6.2	−226.1 ± 19.3	−9.06 ± 0.22	47.2	−80.2 ± 4.3	−229.3 ± 13.7	−9.11 ± 0.18	47.3	−73.3	−208.7	−8.64	46.0
GCUPAGC CGAUUCG	−61.5 ± 5.4	−176.1 ± 17.4	−6.87 ± 0.14	38.7	−67.1 ± 11.2	−194.0 ± 36.1	−6.96 ± 0.18	39.0	−66.2	−189.9	−7.26	40.7
GCUPCGC CGAUGCG	−74.7 ± 3.9	−212.5 ± 12.4	−8.81 ± 0.12	46.7	−74.7 ± 6.9	−212.5 ± 22.0	−8.79 ± 0.10	46.7	−71.7	−202.4	−8.84	47.6
GCUPGGC CGUACCG	−79.7 ± 5.4	−225.1 ± 16.9	−9.90 ± 0.23	50.7	−76.8 ± 10.1	−216.0 ± 31.8	−9.83 ± 0.21	50.9	−73.2	−204.9	−9.64	50.9
GCUPUGC CGAUACG	−53.1 ± 8.5	−150.8 ± 27.2	−6.36 ± 0.39	36.0	−67.8 ± 7.4	−198.1 ± 23.6	−6.37 ± 0.54	36.3	−67.7	−195.8	−6.93	38.9
3′-terminal												
GCGCAP CGCGUU	−55.8 ± 1.9	−160.7 ± 6.1	−5.98 ± 0.03	33.9	−50.4 ± 8.5	−143.0 ± 27.9	−6.00 ± 0.15	33.8	−58.9	−171.0	−5.93	33.7
GCGCCP CGCGGU	−58.3 ± 2.9	−160.3 ± 9.2	−8.62 ± 0.11	48.5	−56.6 ± 6.2	−154.6 ± 19.5	−8.62 ± 0.20	48.9	−60.3	−167.7	−8.27	46.2
GCGCGP CGCGCU	−54.9 ± 2.2	−155.8 ± 7.1	−6.57 ± 0.03	37.2	−49.3 ± 4.6	−137.5 ± 15.1	−6.66 ± 0.18	37.8	−59.3	−166.6	−7.71	43.0
GCGCUP CGCGAU	−63.3 ± 8.8	−182.3 ± 28.4	−6.75 ± 0.33	38.1	−55.0 ± 5.4	−155.5 ± 17.6	−6.79 ± 0.22	38.5	−53.7	−153.7	−6.00	34.0
5′-terminal												
PAGCGC UUCGCG	−58.8 ± 6.0	−163.9 ± 18.9	−7.99 ± 0.23	44.9	−60.9 ± 8.9	−170.7 ± 28.1	−8.00 ± 0.33	44.7	−55.4	−155.9	−7.01	39.8
PCGCGC[c] UGCGCG	−74.8 ± 4.5	−206.1 ± 13.7	−10.87 ± 0.26	56.1	−74.3 ± 5.7	−204.3 ± 17.3	−10.88 ± 0.33	56.3	n/a	n/a	n/a	n/a
PGGCGC UCCGCG	−59.0 ± 6.6	−163.0 ± 20.5	−8.41 ± 0.30	47.2	−57.9 ± 6.4	−159.4 ± 20.1	−8.41 ± 0.20	47.4	−62.4	−170.9	−9.39	51.8
PUGCGC[c] UACGCG	−71.1 ± 7.0	−194.5 ± 21.1	−10.72 ± 0.45	56.4	−73.1 ± 11.7	−200.8 ± 35.8	−10.78 ± 0.62	56.1	n/a	n/a	n/a	n/a

[a]Top strand is written 5′ to 3′, bottom strand is written 3′ to 5′. Solutions are 1 M NaCl, 20 mM sodium cacodylate, 0.5 mM Na_2EDTA, pH = 7.0.
[b]Calculated for 10^{-4} M oligonucleotide concentration.
[c]Two sequences, 5′-PCGCGC-3′/3′-UGCGCG-5′ and 5′-PUGCGC-3′/3′-UACGCG-5′, were excluded from all analyses due to a lack of single, sharp transitions during melting and the possibility of competing unimolecular interactions.
[d]Calculated from nearest neighbor values in Table 3 and Watson–Crick nearest neighbor values (27).

Thermodynamic contribution and nearest neighbor parameters for P●U pairs

The contribution of P●U pairs to duplex thermodynamics is given in Supplementary Table S3. These results include those described by Equations (1) and (2) and the same calculations for enthalpy and entropy. Table 3 lists the nearest neighbor parameters derived for P●U pairs, as described in the Materials and Methods section. All P●U nearest neighbors contribute a negative enthalpy and negative entropy to duplex thermodynamics. $\binom{AP}{UU}$ and $\binom{UP}{AU}$ both have a positive free energy contribution, while all other generated free energy nearest neighbor parameters were negative. The penalty of 0.86 kcal/mol for a terminal P●U pair is twice as destabilizing than the penalty of 0.45 kcal/mol for a terminal A-U pair (29).

The newly derived nearest neighbor parameters were used in conjunction with the nearest neighbor model (29) to give predictive thermodynamic values for duplexes containing P●U pairs. These predicted values can be compared to the experimental values and are given in Table 1. The average deviations between the predicted and experimental values are 4.5%, 5.8% and 6.1% for ΔG°_{37}, ΔH°, and ΔS°, respectively. These deviations are comparable to previous model deviations reported for Watson–Crick (3.2%, 6.0%, and 6.8%, respectively) (29), I●U (5.1%, 4.6%, and 5.1%,

Table 2. Representation of a hydrogen bond; comparison of P•U pairs to A-U pairs in duplexes

oligomers[a]	ΔG°_{37} (kcal/mol)[b]	NN A-U (kcal/mol)[c]	ΔA-U (kcal/mol)[d]	oligomers[a]	ΔG°_{37} (kcal/mol)[b]	NN A-U (kcal/mol)[c]	ΔA-U (kcal/mol)[d]
Internal				*3′-terminal*			
GCAPAGC	−6.95	−8.80	1.85	GCGCAP	−5.98	−7.70	1.72
CGUUUCG				CGCGUU			
GCAPCGC	−8.84	−10.39	1.55	GCGCCP	−8.62	−10.03	1.41
CGUUGCG				CGCGGU			
GCAPGGC	−9.55	−11.13	1.58	GCGCGP	−6.57	−9.37	2.80
CGUUCCG				CGCGCU			
GCAPUGC	−6.99	−9.00	2.01	GCGCUP	−6.75	−8.07	1.32
CGUUACG				CGCGAU			
GCCPAGC	−9.17	−11.13	1.96	Average			1.81
CGGUUCG							
GCCPCGC	−10.94	−12.72	1.78	*5′-terminal*			
CGGUGCG							
GCCPGGC	−12.10	−13.46	1.36	PAGCGC	−7.99	−7.67	−0.32
CGGUCCG				UUCGCG			
GCCPUGC	−9.21	−11.33	2.12	PGGCGC	−8.41	−10.00	1.59
CGGUACG				UCCGCG			
GCGPAGC	−8.99	−10.47	1.48	Average			0.64
CGCUUCG							
GCGPCGC	−10.69	−12.06	1.37				
CGCUGCG							
GCGPGGC	−11.89	−12.80	0.91				
CGCUCCG							
GCGPUGC	−9.06	−10.67	1.61				
CGCUACG							
GCUPAGC	−6.87	−9.17	2.30				
CGAUUCG							
GCUPCGC	−8.81	−10.76	1.95				
CGAUGCG							
GCUPGGC	−9.90	−11.50	1.60				
CGAUCCG							
GCUPUGC	−6.36	−9.37	3.01				
CGAUACG							
Average			1.78				

[a]Top strand is written 5′ to 3′, bottom strand is written 3′ to 5′. Solutions are 1 M NaCl, 20 mM sodium cacodylate, 0.5 mM Na_2EDTA, pH = 7.0.
[b]Measured value for ΔG^{o}_{37} taken from van't Hoff plots.
[c]Predicted using nearest-neighbor parameters for A-U pairs substituted for P·U pairs (27).
[d]Difference between measured ΔG^{o}_{37} values and predicted ΔG^{o}_{37} using A-U pairs in place of P·U pairs where positive values indicate that duplexes containing P·U pairs are less stable than duplexes containing A-U pairs. ΔA-U values represent energy of hydrogen bond.

Table 3. Nearest neighbor parameters for P•U pairs

Nearest Neighbors[a]	Number of Occurrences[b]	ΔH° (kcal/mol)	ΔS° (eu)	ΔG°_{37} (kcal/mol)
AP	5	− 14.0 ± 4.0	− 46.6 ± 12.0	0.43 ± 0.38
UU				
CP	5	− 12.4 ± 4.0	− 37.5 ± 12.0	− 0.76 ± 0.38
GU				
GP	5	− 14.2 ± 4.0	− 42.4 ± 12.0	− 1.10 ± 0.38
CU				
UP	5	− 8.7 ± 4.0	− 29.1 ± 12.0	0.33 ± 0.38
AU				
PA	5	− 10.4 ± 3.7	− 31.3 ± 11.2	− 0.68 ± 0.36
UU				
PC	4	− 15.7 ± 4.5	− 44.2 ± 13.5	− 1.98 ± 0.43
UG				
PG	5	− 14.5 ± 3.7	− 40.7 ± 11.2	− 1.88 ± 0.36
UC				
PU	4	− 11.9 ± 4.5	− 37.4 ± 13.5	− 0.32 ± 0.43
UA				
Terminal P·U	6	2.3 ± 3.0	4.5 ± 9.2	0.86 ± 0.30

[a]For each nearest neighbor pair, the top sequence is written 5′ to 3′ and the bottom sequence is written 3′ to 5′.
[b]The number of times that nearest neighbor pair appears in the sequences studied.

respectively) (1), and Ψ•A (1.7%, 6.7%, and 8.0%, respectively) (2) parameters.

DISCUSSION

Thermodynamic parameters for P•U duplexes

The thermodynamic parameters derived from the optical melting experiments are given in Table 1. An enthalpy agreement of 15% between the average of curve fitting and the van't Hoff plots indicates a two-state transition during melting. All duplexes studied met this criterion. There were, however, two duplexes, ($\frac{PCGCGC}{UGCGCG}$) and ($\frac{PUGCGC}{UACGCG}$), that were excluded from all analyses due to a lack of single, sharp transitions during melting and the possibility of competing unimolecular interactions. For example, the single strand 5′-GCGCGU-3′ could form a duplex with itself consisting of four G-C pairs and two terminal G-U wobble pairs. The melting of the remaining duplexes did show single, sharp transitions and the van't Hoff plots showed a positive correlation between melting temperature and RNA concentration, which suggests duplex formation.

Comparison of duplexes containing P•U pairs and A-U pairs

The stability of duplexes containing P•U pairs was compared to the stability of duplexes containing A-U pairs, and the results can be found in Table 2. The duplexes containing internal P•U pairs were, on average, 1.78 kcal/mol less stable than the corresponding duplexes containing an internal A-U pair. The deletion of the amino group, a hydrogen bond donor, in the P•U pair shows more of a destabilizing effect here than the effect reported for the deletion of the amino group in G-C to I•C pair substitutions (∼1 kcal/mol) (6). This difference may be attributed to cooperative effects between hydrogen bonds within a pair and cooperative effects between neighboring base pairs (9). More specifically, when substituting an I•C pair for a G-C pair, there is a loss of one hydrogen bond but retention of two hydrogen bonds. When substituting a P•U pair for an A-U pair, there is the loss of one hydrogen bond but retention of only one hydrogen bond. The remaining lone hydrogen bond may experience a greater loss of stability due to a cooperativity effect. This greater loss of stability could also be attributed to greater flexibility and rotation of the base due to the lost hydrogen bond. Stacking and hydrogen bonding have been shown to compete in base pairs (10). With only one hydrogen bond holding the P•U pair together, versus two in an A-U pair or I•C pair, the bases may move into an orientation aimed at maximizing the hydrogen bonding strength resulting in weaker stacking interactions. Similarly, the bases could move into an orientation aimed at maximizing the stacking interactions resulting in weaker hydrogen bonding. Structural studies could explain if different orientations are contributing to the destabilization. As of yet, there are no structures in the PDB with a P•U pair surrounded by Watson–Crick pairs.

There are differences in stability for duplexes containing terminal P•U pairs depending on if the P is at the 5′ or 3′ end of the strand. Incorporating a terminal P•U pair with P at the 5′ end of a duplex (see 5′ terminal duplexes in Table 2) was, on average, 0.64 kcal/mol less stable than an A-U pair, while incorporating a terminal P•U pair with P at the 3′ end (see 3′ terminal duplexes in Table 2) was, on average, 1.81 kcal/mol less stable than the corresponding duplex with an A-U pair. This result shows differences based on position within the helix that can be attributed to differences in stacking. This result is similar to results seen in the G-C to I•C pair substitutions where a hydrogen bond is worth −1.6 kcal/mol or −0.7 kcal/mol depending on whether the I is the at the 5′ or 3′ end (10). Again, without structural information, it is hard to determine the source of the differences seen here.

Nearest neighbor parameters for P•U pairs

Similar to nearest neighbor trends for Watson–Crick/Watson–Crick pairs, all derived enthalpy and entropy nearest neighbor parameters for P•U pairs are negative. Conversely, the derived free energy nearest neighbor parameters have both positive and negative parameters, ranging from −1.94 kcal/mol to 0.39 kcal/mol. Both $\binom{AP}{UU}$ and $\binom{UP}{AU}$ contribute a positive, unfavorable, term to duplex ΔG°_{37}. This has been seen for previously derived free energy parameters for I•U pairs, both $\binom{UI}{AU}$ and $\binom{IA}{UU}$ contributed a positive term to duplex ΔG°_{37} (1). These nearest neighbor combinations are similar to the $\binom{AA}{UU}$ and $\binom{UA}{AU}$ nearest neighbor combinations, two of the least stabilizing Watson–Crick nearest neighbor parameters. It is not surprising that when a hydrogen bond is removed (when A is replaced by P), the nearest neighbor parameters become destabilizing. It is important to remember, however, that the incorporation of a P•U pair into a non-terminal position in a duplex involves two nearest neighbor parameters involving P•U. Therefore, the contribution of one of these nearest neighbor parameters will be summed with a second P•U nearest neighbor parameter. In almost all cases, this will result in a stabilizing contribution from the inclusion of a P•U pair.

The general trend when A-U is the 3′ pair in a nearest neighbor combination from most stable to least stable is $\binom{GA}{CU} > \binom{CA}{GU} > \binom{UA}{AU} > \binom{AA}{UU}$ (20). This is the same trend for when a P•U pair is the 3′ pair in a nearest neighbor combination, or $\binom{GP}{CU} \approx \binom{CP}{GU} > \binom{UP}{AU} \approx \binom{AP}{UU}$. The similarity of stability trends between Watson–Crick pairs and P•U pairs can also be seen when a P•U pair is the 5′ pair in a nearest neighbor combination, $\binom{PC}{UG} \approx \binom{PG}{UC} > \binom{PA}{UU} \approx \binom{PU}{UA}$, except here, the two least stable nearest neighbor parameters are switched from their Watson–Crick counterparts (although the P•U parameters in question are within experimental error of each other). In both instances where a P•U pair is in a nearest neighbor combination, the nearest neighbors with a G-C pair are more stable than the nearest neighbors with an A-U pair, as is seen for canonical pairs (29). This is likely due to the extra hydrogen bond in a G-C pair versus an A-U pair. Also, each P•U nearest neighbor combination contributes less to duplex stability than the corresponding A-U nearest neighbor pair. This result is consistent with the decrease in stability due to the removal of a hydrogen bond. It is also possible that differences in stacking contribute to the differences between P•U nearest neighbor combinations containing G-C pairs versus A-U pairs and contribute to the differences between P•U nearest neighbor combinations versus A-U nearest neighbor combinations.

It is also noted that the ΔG°_{37} term is more negative (i.e. more stable) when the P•U pair is the 5′ pair in a nearest neighbor combination, or $\binom{PN}{UN}$, than when the P•U pair is the 3′ pair, or $\binom{NP}{NU}$. This result is similar to results seen with A•A mismatches where A was replaced with P giving P•A pairs (7). Although the P is paired with A instead of U, the duplex with the P•A as the 5′ pair or $\binom{PA}{AA}$, showed an increase in stability and the duplex with P•A as the 3′ pair,

or ($\begin{matrix} AP \\ AA \end{matrix}$), showed a decrease in stability in comparison to the A•A mismatch (7). However, some of this difference for P•A pairs may be attributed to differing base pair orientations, as the hydrogen bonding is *trans* Hoogsteen/sugar-edge for the P•A pair and *trans* Watson–Crick/Watson–Crick for the A•P pair (7).

Value of a hydrogen bond

The effect on the stability of RNA duplexes reported for hydrogen bonds can vary depending on the location and type of the hydrogen bond. Table 4 summarizes the free energy differences in duplexes from the literature where nucleobase replacements have removed hydrogen bonds (31). The results in Table 2 give energy differences equivalent to the loss of a hydrogen bond in the context of duplexes where an A-U pair was replaced with a P•U pair. The values included in Table 4 for the duplexes with a P•U pair replacement are the average values given in Table 2. Position in the helix, number of hydrogen bonds, and type of hydrogen bond play a role in contributing to duplex stability. For example, 2,6-diaminopurine (D)•U and G-C pairs have the same number but different type of hydrogen bonds. G-C and A-U pairs have different number and different type of hydrogen bonds, and A-U and P•U pairs have different number but same type of hydrogen bonds, as do G-C and I•C pairs.

The free energy value of a hydrogen bond, given in Table 4, ranges from −0.4 to −3.4 kcal/mol. The free energy value of a hydrogen bond in a P•U pair with various nearest neighbor combinations, given in Table 2, is similar and ranges from 0.3 to −3.0 kcal/mol. Also, the effect of a hydrogen bond on the stability of a duplex is similar for DNA versus RNA. The energy values for a hydrogen bond in duplexed DNA versus duplexed RNA range from −0.5 to −1.8 kcal/mol and −0.4 to −1.9 kcal/mol, respectively.

Still, with these similarities there are differences. For example, the range for the value of a hydrogen bond in RNA hairpins is −1.8 to −3.4 kcal/mol, whereas the range for duplexed RNA is −0.4 to −1.9 kcal/mol. Also, there is a difference in energy when an A-U pair replaces a G-C pair depending on the location of the base pair and the sequence composition of the duplex. If the replacement occurs at the end of a duplex with a -GCGC- core, the hydrogen bond value is −0.5 kcal/mol (entry 8 of Table 4). If the replacement occurs at the end of a duplex with an -AUGCAU- core, the hydrogen bond value is −1.5 kcal/mol (entry 9 of Table 4). This difference is large considering that both duplexes have a G-C to A-U replacement at the helix termini. However, if the replacement (G-C to A-U) occurs at the center of a duplex, the hydrogen bond value is −1.6 kcal/mol (entry 7 of Table 4) or −1.9 kcal/mol (entry 11 of Table 4) depending on the sequence composition. Here, the difference is relatively small.

The internal and terminal average values from this work are included in Table 4 as entries 15, 16, and 17. All internal replacements for duplexed RNA without P•U pairs range from −1.5 kcal/mol to −1.9 kcal/mol (Table 4). The average value for internal A-U to P•U pair replacement is −1.8 kcal/mol (entry 17 of Table 4), which is within the range for internal replacements for duplexed RNA without P•U pairs. Although this average value falls within the range observed for internal replacements of duplexed RNA without P•U pairs, there is variation in the individual values for internal A-U to P•U pair replacement, and some of the individual values (Table 2) are outside of this range.

On the other hand, all terminal replacements for RNA without P•U pairs (entries 1, 2, 4, 5, 8, and 9 of Table 4) range from −0.4 kcal/mol to −1.6 kcal/mol. The terminal average values for duplexes with A-U to P•U pair replacement (entries 15 and 16 of Table 4) are −1.8 kcal/mol for the terminal pair with the 3′ P and −0.6 kcal/mol for the terminal pair with the 5′ P. Although the value for the terminal pair with the 5′ P is within the range observed for terminal replacements of RNA without P•U pairs, the value for the terminal pair with the 3′ P is not. The range of values for these entries highlights the effects from not only the location within a duplex, but also the neighboring base pairs, on the value of a hydrogen bond. The type of hydrogen bonds can also have an effect on the value of a hydrogen bond. A G-C to A-U replacement at the terminus of a duplex results in a pair with three hydrogen bonds being replaced by a pair with two hydrogen bonds, just as in a D•U to A-U replace-

Table 4. Comparison of duplexes with different number of hydrogen bonds

Polymer Type[b]	Reference Duplex[c]	Duplex with fewer H bonds[d]	Differences in No. of H Bonds	$\Delta\Delta G°_{37}$/H Bond (kcal/mol H Bond)	Reference
RNA	GCCGGC CGGCCG	ICCGGC CGGCCI	2	-1.6	10
	CGGCCG GCCGGC	CGGCCI ICCGGC	2	-0.7	10
	CGGCCG GCCGGC	CAGCUG GUCGAC	2	-1.6	12
	GCCGGC CGGCCG	ACCGGU UGGCCA	2	-1.4	12
	DCCGGU UGGCCD	ACCGGU UGGCCA	2	-0.4	13
	GCGCGC CGCGCG	GUGCAC CACGUG	2	-1.5	12
	GCGCGC CGCGCG	GCAUGC CGUACG	2	-1.6	12
	CGCGCG GCGCGC	UGCGCA ACGCGU	2	-0.5	12
	GAUGCAUC CUACGUAG	AAUGCAUU UUACGUAA	2	-1.5	12
	AUGCGCAU UACGCGUA	AUACGUAU UAUGCAUA	2	-1.8	12
	AUGCGCAU UACGCGUA	AUGUACAU UACAUGUA	2	-1.9	12
	GACGACUCU$_4$GAGUCGUC	GACIACUCU$_4$GAGUCGUC	1	-3.4	9
	GACGACUCU$_4$GAGUCGUC	GACGACUCU$_4$GAIUCGUC	1	-2.6	9
	GGCGCAAGCC	GGCGCAAICC	1	-1.8	11
	GCGCNA CGCGNU	GCGCNP CGCGNU	1	-1.8	this work[e]
	ANGCGC UNCGCG	PNGCGC UNCGCG	1	-0.6	this work[e]
	GCNANGC CGNUNCG	GCNPNGC CGNUNCG	1	-1.8	this work[e]
DNA	dCA$_3$GA$_3$G dGT$_3$CT$_3$C	dCA$_3$IA$_3$G dGT$_3$CT$_3$C	1	-0.5	32
	dCA$_3$CA$_3$G dGT$_3$GT$_3$C	dCA$_3$CA$_3$G dGT$_3$IT$_3$C	1	-1.8	33
	dG$_3$A$_2$GCT$_2$C$_3$ dC$_3$T$_2$CGA$_2$G$_3$	dG$_3$A$_2$ICT$_2$C$_3$ dC$_3$T$_2$CIA$_2$G$_3$	2	-1.3	34
	dCGTDCG dGCDTGC	dCGTACG dGCATGC	2	-0.5	35

[a]Table adapted from ref. (31). [b] Entires with two strands form duplexes, and entries with one strand form a hairpin. Duplexes are written with the top strand 5' to 3' and the bottom strand 3' to 5'; hairpins are written 5' to 3'.
[c] D is 2,6-diaminopurine. [d] Blue font highlights changes from reference duplex. I is inosine. [e] $\Delta\Delta G°_{37}$ is the average values listed in Table 2.

ment. Yet, the value for a terminal G-C to A-U replacement is −1.4 kcal/mol (entry 4 of Table 4) and the value for a terminal DA•U replacement is −0.4 kcal/mol (entry 5 of Table 4). The type of hydrogen bond having an effect on the value of the hydrogen bond is even further highlighted when comparing an A-U pair to a 2-aminopurine•U pair. Here, the number of hydrogen bonds has not changed but the type of hydrogen bonds has changed. An RNA hairpin where an A-U to 2-aminopurine•U pair replacement occurred at the stem region had a difference in free energy of 0.8 kcal/mol (8). The range of values found in Tables 2 and 4 suggests that a single value representing the energy of a hydrogen bond may be insufficient for understanding the contribution to duplex stability by functional groups that participate in hydrogen bonds.

The results of this study indicate that duplexes containing P•U pairs are less stable than the same duplexes containing A-U pairs, which is as expected. The derived nearest neighbor parameters can be used in structure prediction software to determine the stability of RNA duplexes containing P•U pairs. These results highlight the destabilization to a duplex upon the loss of one hydrogen bond. The destabilization effect can vary depending on the location within the duplex and the nearest neighbors to the P•U pair. Structural studies or computational studies may further explain the source of the destabilization due to P•U pair substitution.

SUPPLEMENTARY DATA

Supplementary Data are available at NAR Online.

FUNDING

National Institutes of Health (NIH) [2R15GM085699-02]. Funding for open access charge: National Institutes of Health (NIH) [2R15GM085699-02].
Conflict of interest statement. None declared.

REFERENCES

1. Wright,D.J., Rice,J.L., Yanker,D.M. and Znosko,B.M. (2007) Nearest neighbor parameters for inosine•uridine pairs in RNA duplexes. *Biochemistry*, **46**, 4625–4634.
2. Hudson,G.A., Bloomingdale,R.J. and Znosko,B.M. (2013) Thermodynamic contribution and nearest-neighbor parameters of pseudouridine•adenosine base pairs in oligoribonucleotides. *RNA*, **19**, 1474–1482.
3. Richardson,K.E. and Znosko,B.M. (2016) Nearest-neighbor parameters for 7-deaza-adenosine•uridine base pairs in RNA duplexes. *RNA*, **22**, 934–942.
4. Silverman,S.K. and Cech,T.R. (1999) Energetics and cooperativity of tertiary hydrogen bonds in RNA structure. *Biochemistry*, **38**, 8691–8702.
5. Nakano,S. and Sugimoto,N. (2014) Roles of the amino group of purine bases in the thermodynamics stability of DNA base pairing. *Molecules*, **19**, 11613–11627.
6. Grohman,J.K., Gorelick,R.J., Lickwar,C.R., Lieb,J.D., Bower,B.D., Znosko,B.M. and Weeks,K.M. (2013) A guanosine-centric mechanism for RNA chaperone function. *Science*, **340**, 190–195.
7. Znosko,B.M., Burkard,M.E., Krugh,T.R. and Turner,D.H. (2002) Molecular recognition in purine-rich internal loops: Thermodynamic, structural, and dynamic consequences of purine for adenine substitutions in 5′(rGGCAAGCCU)$_2$. *Biochemistry*, **41**, 14978–14987.
8. Dishler,A.L., McMichael,E.L. and Serra,M.J. (2015) Determination of the secondary structure of group II bulge loops using fluorescent probe 2-aminopurine. *RNA*, **21**, 975–984.
9. Siegfried,N.A., Metzger,S.L. and Bevilacqua,P.C. (2007) Folding cooperativity in RNA and DNA is dependent on position in the helix. *Biochemistry*, **46**, 172–181.
10. Turner,D.H., Sugimoto,N., Kierzek,R. and Dreiker,S.D. (1987) Free energy increments for hydrogen bonds in nucleic acid base pairs. *J. Am. Chem. Soc.*, **109**, 3783–3785.
11. SantaLucia,J. Jr, Kierzek,R. and Turner,D.H. (1992) Context dependence of hydrogen bond free energy revealed by substitutions in an RNA hairpin. *Science*, **256**, 217–219.
12. Freier,S.M., Sugimoto,N., Sinclair,A., Alkema,D., Neilson,T., Kierzek,R., Caruthers,M.H. and Turner,D.H. (1986) Stability of XGCGCp, GCGCYp, and XGCGCYp helixes: An empirical estimate of the energetics of hydrogen bonds in nucleic acids. *Biochemistry*, **25**, 3214–3219.
13. Strobel,S.A., Cech,T.R., Usman,N. and Beigelman,L. (1994) The 2, 6-diaminopurine riboside•5-methylisocytodine wobble base pair: An isoenergetic substitution for the study of G•U pairs in RNA. *Biochemistry*, **33**, 13824–13835.
14. Gillerman,I. and Fischer,B. (2011) Investigations into the origins of the molecular recognition of several adenosine deaminase inhibitors. *J. Med. Chem.*, **54**, 107–121.
15. Shewach,D.S., Krawczyk,S.H., Acevedo,O.L. and Townsend,L.B. (1992) Inhibition of adenosine deaminase by azapurine ribonucleosides. *Biochem. Pharmacol.*, **44**, 1697–1700.
16. Véliz,E., Easterwood,L.M. and Beal,P.A. (2003) Substrate analogues for an RNA-editing adenosine deaminase: Mechanistic investigation and inhibitor design. *J. Am. Chem. Soc.*, **125**, 10867–10876.
17. Haudenschild,B.L., Maydanovych,O., Véliz,E., Macbeth,M.R., Bass,B.L. and Beal,P.A. (2004) A transition state analogue for an RNA-editing reaction. *J. Am. Chem. Soc.*, **126**, 11213–11219.
18. Maydanovich,O. and Beal,P.A. (2006) C6-substituted analogues of 8-azanebularine: Probes of an RNA-editing enzyme active site. *Org. Lett.*, **8**, 3753–3756.
19. Slim,G. and Gait,M.J. (1992) The role of the exocyclic amino groups of conserved purines in hammerhead ribozyme cleavage. *Biochem. Biophys. Res. Commun.*, **183**, 605–609.
20. Fu,D.J. and McLaughlin,L.W. (1992) Importance of specific purine amino and hydroxyl groups for efficient cleavage by a hammerhead ribozyme. *Proc. Natl. Acad. Sci. U.S.A.*, **89**, 3985–3989.
21. Fu,D.J., Rajur,S.B. and McLaughlin,L.W. (1993) Importance of specific guanosine N^7-nitrogen and purine amino groups for efficient cleavage by a hammerhead ribozyme. *Biochemistry*, **32**, 10629–10637.
22. Blount,K.F. and Uhlenbeck,O.C. (2005) The structure-function dilemma of the hammerhead ribozyme. *Annu. Rev. Biophys. Biomol. Struct.*, **34**, 415–440.
23. Addepalli,H., Meena, Peng,C.G., Wang,G., Fan,Y., Charisse,K., Hayaprakash,K.N., Rajeev,K.G., Pandey,R.K., Lavine,G. *et al.* (2010) Modulation of thermal stability can enhance the potency of siRNA. *Nucleic Acids Res.*, **38**, 7320–7331.
24. Mathews,D.H. (2004) Using an RNA secondary structure partition function to determine confidence in base pairs predicted by free energy minimization. *RNA*, **10**, 1178–1190.
25. McDowell,J.A. and Turner,D.H. (1996) Investigations of the structural basis for thermodynamic stabilities of tandem GU mismatches: Solution structure of (rGAGGUCUC)$_2$ by two-dimensional NMR and simulated annealing. *Biochemistry*, **35**, 14077–14089.
26. Chen,G., Kennedy,S.D., Qiao,J., Krugh,T.R. and Turner,D.H. (2006) An alternating sheared AA pair and elements of stability for a single sheared purine-purine pair flanked by sheared GA pairs in RNA. *Biochemistry*, **45**, 6889–6903.
27. Petersheim,M. and Turner,D.H. (1983) Base-stacking and base-pairing contributions to helix stablility: Thermodynamics of double-helix formation with CCGG, CCGGp, mCCGGAp, ACGGP, CCGGUp, and ACCGGUp. *Biochemistry*, **22**, 256–263.
28. Borer,P.N., Dengler,B., Tinoco,I. and Uhlenbeck,O. (1974) Stability of ribonucleic-acid double-stranded helices. *J. Mol. Biol.*, **86**, 843–853.
29. Xia,T., SantaLucia,J. Jr, Burkard,M.E., Kierzek,R., Schroeder,S.J., Jiao,X., Cox,C. and Turner,D.H. (1998) Thermodynamic parameters for an expanded nearest-neighbor model for formation of RNA duplexes with Watson-Crick base pairs. *Biochemistry*, **37**, 14719–14735.

30. Schroeder,S.J. and Turner,D.H. (2009) Optical meting measurements of nucleic acid thermodynamics. In: Herschlag,D (ed). *Methods in Enzymology*. Academic Press, Burlington, Vol. **468**, pp. 371–387.
31. Turner,D.H. (2000) Conformation changes. In: Bloomfield,V.A., Crothers,D.M. and Tinoco,I. Jr (eds). *Nucleic acids, structure, properties, and functions*. University Science Books, Sausalito, pp 259–334.
32. Martin,F.H., Castro,M. M., Aboul-ela,F. and Tinoco,I. Jr (1985) Base pairing involving deoxyinosine: Implications for probe design. *Nucleic Acids Res.*, **13**, 8927–8938.
33. Aboul-ela,F., Koh,D., Tinoco,I. Jr and Martin,F.H. (1985) Base-base mismatches. Thermodynamics of double helix formation for $dCA_3XA_3G + dCT_3YT_3G$ (X, Y=A, C, G, T). *Nucleic Acids Res.*, **13**, 4811–4824.
34. Kawase,S., Iwai,S., Inoue,H., Miura,K. and Ohtsuka,E. (1986) Studies on nucleic acid interactions I. Stabilities of mini-duplexes ($dG_2A_4XA_4G_2.dC_2T_4YT_4C_2$) and self-complementary d(GGGAAXYTTCCC) containing deoxyinosine and other mismatched bases. *Nucleic Acids Res.*, **14**, 7727–7736.
35. Gaffney,B.L., Marky,L.A. and Jones,R.A. (1984) The influence of the purine 2-amino group on DNA conformation and stability-II. Synthesis and physical characterization of d[CGT(2-NH_2)ACG], d[CGU(2-NH_2)ACG], and d[CGT(2-NH_2)AT(2-NH_2)ACG]. *Tetrahedron*, **40**, 3–13.